1 **Revision 1**, Word Count: 6291

2 EntraPT: an online platform for elastic geothermobarometry

3 Mattia Luca Mazzucchelli[1], Ross John Angel[2], Matteo Alvaro[1]

4 [1]Department of Earth and Environmental Sciences, University of Pavia, Via A. Ferrata, 1, Pavia,

5 27100, Italy

6 [2]IGG-CNR, Via G. Gradenigo 6, Padova, 35131, Italy

7 Corresponding author: Mattia L. Mazzucchelli (mattialuca.mazzucchelli@unipv.it)

8

9 Abstract

10 EntraPT is a web-based application for elastic geobarometry freely accessible at the "Fiorenzo
11 Mazzi" experimental mineralogy lab website (www.mineralogylab.com/software). It provides an
12 easy-to-use tool to calculate the entrapment conditions of inclusions, with error propagation, from
13 the residual strain measured in mineral inclusions. EntraPT establishes a method and a workflow
14 to import and analyze the measured residual strains, correctly calculate the mean stress in the
15 inclusions, compute the entrapment isomekes with uncertainty estimation, and visualize all the
16 results in relevant graphs. It enables the user to avoid the many possible errors that can arise from
17 manual handling of the data, and from the numerous steps required in geobarometry calculations.
18 All of the data, parameters and settings are stored in a consistent format and can be exported as
19 project files and spreadsheets, and imported back to EntraPT for further analysis. This allows
20 researchers to store and/or share their data easily, making the checking and the comparison of data
21 and results reliable. EntraPT is an online tool that does not require any download and/or

installation, and it will be updated in the future with new functionalities made available from advances in the development of elastic geobarometry.

Keywords: EntraPT program, elastic geothermobarometry, host-inclusion systems, elasticity

Introduction

Mineral inclusions entrapped in their mineral hosts have provided fundamental information on geological processes, first through simple phase identification (e.g. Chopin 1984). More recently, advances in mineral physics data and the widesperead availability of analysis tools such as Raman spectrometers has resulted in the rapid development of the field of piezobarometry for a wide range of geological settings. Residual strains are developed in inclusions because of the contrast between their elastic properties and those of their host. If the residual strain is measured and interpreted correctly, the conditions at entrapment ($\boldsymbol{P_{trap}}$, $\boldsymbol{T_{trap}}$) can be determined by using the elastic properties of the host and the inclusion. The basic concept has been known for a long time (e.g. Rosenfeld and Chase 1961; Gillet et al., 1984; Izraeli et al., 1999; Zhang, 1998). Current applications are based on the assumptions that both the host and inclusion minerals are elastically isotropic and that the inclusion is an isolated sphere. Under such conditions the stress in the inclusion will be a hydrostatic pressure. It can be determined by measuring the shift of the Raman lines of the inclusion, or the unit-cell volume of the inclusion by diffraction. In absence of plastic or viscous deformation (e.g. Zhong et al., 2018; Zhong et al., 2020), the determination of possible entrapment conditions, the entrapment isomeke, is then a straight-forward calculation that is implemented in a number of freeware programs such as EosFit7c (Angel et al., 2014a), EosFit-

Pinc (Angel et al., 2017a), QuIB-calc (Ashley et al., 2014), or the algorithm published in Kohn (2014).

However, no mineral crystal is elastically isotropic, and no inclusion is a perfect isolated sphere. As a consequence the stress field inside the inclusion is not hydrostatic when the host is in the laboratory (Eshelby, 1959; Murri et al., 2018; Mazzucchelli et al., 2018; Mazzucchelli et al., 2019). The shifts of Raman lines of the inclusion are therefore different from those under hydrostatic conditions (e.g. Anzolini et al., 2018; Thomas and Spear, 2018). Using hydrostatic calibrations of Raman shifts (e.g. Enami et al., 2007; Ashley et al., 2016) can lead to significantly inaccurate estimates of the residual "pressure" in the inclusion and, in turn, of the entrapment conditions, leading to fundamental misinterpretations of geological processes. The shifts of Raman lines of inclusions are correctly interpreted through the mode Grueneisen tensors of the inclusion crystal (e.g. Grüneisen, 1926; Barron et al., 1980; Angel et al., 2019). These tensors allow the strains of the inclusion crystal relative to a free crystal to be determined from the measured Raman shifts. Or, the strains can be determined by direct in-situ difraction measurements of the inclusion (e.g. Nestola et al., 2011; Alvaro et al., 2020). Once the strains are determined, the residual stress and the residual pressure in the inclusion can be determined via the elastic tensor. Bonazzi et al. (2019) showed that the entrapment conditions of synthetic quartz inclusions can be determined in this way even in presence of deviatoric stress.

The determination of reliable geological conditions of inclusion entrapment from non-spherical anisotropic inclusions is thus far more complex, involving several intermediate steps with tensor calculations, than the isotropic approach embodied in existing software. Shape corrections are made with the relaxation tensor of the inclusion which, for non-ellipsoidal inclusions or anisotropic hosts, must be determined with numerical calculations such as finite element modeling

(Mazzucchelli et al., 2018; Mazzucchelli et al., 2019; Morganti et al., 2020; Alvaro et al., 2020). Therefore, we have developed EntraPT, a web application which implements the methods developed by Angel et al. (2019) and Murri et al. (2018) and applied by Bonazzi et al. (2019), to correctly calculate the mean stress in inclusions from the measured strains, and then to calculate entrapment isomekes with the isotropic model including the propagation of uncertainties. EntraPT is freely accessible after registration. It can be used to process strain data from a single inclusion or large datasets of residual strains of multiple inclusions to obtain entrapment conditions and to easily generate plots. In this paper we introduce the EntraPT program, document its methods and illustrate its functionalities. A guided example of a step-by-step analysis of a dataset of quartz inclusions entrapped in almandine (Bonazzi et al., 2019) is provided in the Supplementary material.

Program description

The successful determination of the *P-T* of metamorphism using elastic geothermobarometry ideally requires the analysis of a large number of inclusions (e.g. Bonazzi et al., 2019). Because of the contrast in elastic properties between the two minerals, some host-inclusion systems are good geothermometers (e.g. zircon in garnet) while other are good barometers (e.g. quartz in garnet), and their coexistence in the same rock might provide a constraint on the metamorphic *P-T* path of the rock, because of the different slopes of their isomekes (e.g. Zhong et al., 2019). Furthermore, to interpret correctly the conditions of metamorphism it is necessary to account for all of the uncertainties from the measurement of the residual strain to the calculation of the entrapment conditions. EntraPT is a MATLAB® based online application with a Graphical User Interface (GUI) that can be used to (see Fig. 1): (1) import and visualize the residual strain and the associated

89 uncertainties from measurements in inclusions (Fig 1c-f); (2) correctly calculate the mean stress
90 in inclusions from the measured strains (Fig. 1g); (3) calculate entrapment isomekes with the
91 isotropic model of Angel, et al. (2017a) with uncertainty propagation; (4) plot the entrapment
92 isomekes for multiple inclusions simultaneously (Fig. 1h); (5) export all the data and results as
93 project files or spreadsheets to store and share them (Fig. 1i).
94 EntraPT is freely accessible upon registration as an online application at the website of the
95 "Fiorenzo Mazzi" Experimental Mineralogy Lab (www.mineralogylab.com/software). EntraPT is
96 supported on most of the common browsers and operating systems (Windows®, macOS®,
97 Linux®) and no download and/or installation is required. The app was developed with
98 MATLAB® AppDesigner and deployed with the MATLAB® Compiler on Web App Server. For
99 all of the calculations based on the equations of state (EoS) of the minerals (e.g. the calculation of
100 the residual pressure and of the entrapment isomeke), EntraPT relies on Eosfit7 (Angel et al.,
101 2014a) a stable and efficient Fortran code that has been validated over many years. Eosfit7n, a
102 fast version of the program without a console or GUI for direct user interaction, is embedded in
103 EntraPT. The instructions and EoS parameters for calculations are sent from EntraPT to Eosfit7n
104 as files. Once the calculations are terminated, the output generated by Eosfit7n is read back into
105 EntraPT. The use of EosFit7n as a separate executable ensures that in the future EntraPT will be
106 able to access new EoS forms and other developments introduced into the CrysFML library
107 (Rodriguez-Carvajal and González-Platas, 2003) and EosFit program suite.
108
109 The user interface of EntraPT consists of three main tabs: *Add New Analyses*, *Calculate*
110 *Entrapment* and *View Data* (Fig. 2a, b, c) designed to guide the user through the required work
111 path. The workflow, from the definition of the host-inclusion system to the calculation of

112 entrapment conditions and the data visualization, is illustrated in detail in the Supplementary
113 material, taking as an example the dataset of quartz inclusions entrapped in almandine reported by
114 Bonazzi et al. (2019). EntraPT works on *analyses*. Each *analysis* is a container of all of the
115 information relative to one measurement of residual strain and the calculations performed on it.
116 An *analysis* is defined at least by:

117 • A label
118 • A pair of mineral phases: the host and the inclusion phase
119 • The elastic properties of the host and the inclusion (EoS, stiffness tensors)
120 • The geometry of the host-inclusion system
121 • The relative orientation between the host and the inclusion
122 • The residual strain state defined by the components of residual strain vector, and its
123 covariance matrix

124 Other data that can be optionally associated with an *analysis* are:

125 • The labels of the sample, thin section, host, inclusion and of the point analysis
126 • A text description
127 • The results of the calculation of its entrapment conditions (i.e. P and T of the entrapment
128 isomeke, and all the intermediate results, such as residual stress, unrelaxed strain, their
129 covariance matrices, etc..)

130 With this definition, two measurements of residual strain taken in the same inclusion crystal are
131 stored and treated as separate *analyses* in EntraPT. In fact, even if they belong to the same host-
132 inclusion system (same mineral phases, geometry and orientation) they can differ in the residual
133 strain. For the same reason, measurements from several inclusions in the same host crystal are also
134 considered as separate *analyses*. This allows for great flexibility in storing and processing the

measurements, since each of them can have different data and metadata and can be handled separately.

EntraPT makes use of the Voigt notation (Voigt, 1910) to represent tensors, and this notation will be assumed thoughout this paper. Therefore 2^{nd} rank tensors are represented as vectors and 4^{th} rank tensors as matrices. The mapping of the indices between the tensor notation and the vector (Voigt) notation is the following:

Tensor notation	11	22	33	23	13	12
Voigt notation	1	2	3	4	5	6

Properties of the host-inclusion system

In EntraPT the user first adds one or more new *analyses* to the project from the *Add New Analyses* tab (Fig. 2a), where the host and the inclusion minerals, the geometry of the system and their relative orientation must be chosen. The calculation of the entrapment conditions requires the elastic properties of the minerals. EntraPT is based on an internally-consistent database of elastic properties (Table 1). The database contains for each mineral phase the volume EoS and, for inclusions, the 4^{th} rank elastic tensor at room conditions. The elastic tensors are taken from experimental determinations reported in the literature, and, if necessary, their components are rescaled to ensure that the Reuss bulk modulus equals that of the volume EoS (Table 1) at room conditions. This ensures consistency throughout the entire calculation. During the rescaling, care is taken that the degree of anisotropy (evaluated through the Universal anisotropic index, Ranganathan and Ostoja-Starzewski, 2008) is not altered (see Mazzucchelli et al., 2019 for further details). Only phases with published and validated elastic properties and EoS are included in the

program database. In the current version aluminosilicate garnet endmembers (e.g. pyrope, almandine and grossular) and diamond are available as hosts. The inclusion can be chosen among quartz, zircon, diamond and garnet. Addtional hosts and inclusion minerals will be added as further internally consistent elastic data and EoS become available.

Residual strain

Once the properties of the system are set, the user must input the residual strain measured in the inclusion for each *analysis* (Fig. 2g). As shown by Murri et al. (2019) and Angel et al. (2019) the strain state can be obtained from the measured Raman shifts by applying the concept of the phonon-mode Gruneisen tensor. This can be done easily for inclusions such as quartz and zircon using stRAinMAN (Angel et al., 2019), a free program that can be downloaded at http://www.rossangel.com/. stRAinMAN allows the user to load the measured Raman shifts and to export the resulting strain components and the associated standard deviations and correlations in a logfile. For a uniaxial inclusion without symmetry breaking, stRAinMAN provides an output with the sum of the strain components (in Voigt notation) $\varepsilon_1 + \varepsilon_2$, the component ε_3, their estimated standard deviations (esd) and the covariance between $\varepsilon_1 + \varepsilon_2$ and ε_3. If the strain is measured with X-ray diffraction, measurements need to be carefully interpreted because irregular and faceted inclusions may exhibit stress and strain gradients. In this case, diffraction measurements only provide some average value of strain over the whole inclusion volume that cannot be used directly in elastic geobarometry (e.g. Campomenosi et al., 2018; Mazzucchelli et al., 2018; Murri et al., 2018, Alvaro et al., 2020). However, with XRD the value of each strain component (together with their esd and covariances) can be determined independently.

The user can input the components of the residual strain and the associated uncertainties into EntraPT, for each *analysis*. The esd's and the covariances associated with the residual strains are needed to propagate the uncertainties into the residual pressure and the entrapment isomeke. Since the application of elastic geobarometry usually requires the processing of several measurements performed on several inclusions, the user has the option of importing a text file with a list of *analyses* with their strains and the associated uncertainties. The input file can be selected with a file-browser window and it is uploaded to the server via a secure SSL connection. This procedure, applied to the data of Bonazzi et al. (2019), is described in detail in the Supplementary material and shown in Fig. S2. Template files are provided with the program on the website mineralogylab.com that can be edited with a spreadsheet editor, to preserve the tab delimited structure. Each row of this file stores the data of one *analysis*, i.e. of one measurement. All of the *analyses* in one input file must belong to the same host-inclusion system (i.e. same host and inclusion phases). The file format allows each *analysis* to be identified (sample, thin section, host, inclusion and point analysis) and notes associated to the *analysis* to be recorded. The content of the remaining columns depends on the symmetry of the residual strain, which corresponds to the symmetry of the inclusion in absence of symmetry breaking (see Table S1 in the Supplementary material and the **.dat* file included in the Deposit items for an example). The measured strain components and the statistical parameters (esd, covariances) can be easily copied and pasted from the stRAinMAN logfile to this input file using any spreadsheet editor. During the import process, EntraPT checks that the file is readable and that the data are consistent. Depending on the symmetry of the inclusion selected by the user in the app, a minimum number of independent strain components is required. Moreover, the symmetry of the inclusion prescribes the equality between some of the components of the strain. A check is also performed on the consistency of the provided

esd and covariances, since the resulting covariance matrix must be positive definite. Analyses that do not satisfy these requirements are discarded during the import process, and a detailed message describing the errors is shown to the user. EntraPT requires the full 6 x 6 covariance matrix $\boldsymbol{V}^{\varepsilon}$ of the residual strain values in order to propagate the uncertainties through the calculations of the residual pressure and the entrapment isomeke. For a general state of residual strain with six independent components in Voigt notation $(\varepsilon_1, \varepsilon_2, \varepsilon_3, \varepsilon_4, \varepsilon_5, \varepsilon_6)$, the fully-symmetric covariance matrix $\boldsymbol{V}^{\varepsilon}$ is defined as:

$$\boldsymbol{V}^{\varepsilon} = \begin{bmatrix} esd(\varepsilon_1)^2 & cov(\varepsilon_1,\varepsilon_2) & cov(\varepsilon_1,\varepsilon_3) & cov(\varepsilon_1,\varepsilon_4) & cov(\varepsilon_1,\varepsilon_5) & cov(\varepsilon_1,\varepsilon_6) \\ & esd(\varepsilon_2)^2 & cov(\varepsilon_2,\varepsilon_3) & cov(\varepsilon_2,\varepsilon_4) & cov(\varepsilon_2,\varepsilon_5) & cov(\varepsilon_2,\varepsilon_6) \\ & & esd(\varepsilon_3)^2 & cov(\varepsilon_3,\varepsilon_4) & cov(\varepsilon_3,\varepsilon_5) & cov(\varepsilon_3,\varepsilon_6) \\ & & & esd(\varepsilon_4)^2 & cov(\varepsilon_4,\varepsilon_5) & cov(\varepsilon_4,\varepsilon_6) \\ & Symmetric & & & esd(\varepsilon_5)^2 & cov(\varepsilon_5,\varepsilon_6) \\ & & & & & esd(\varepsilon_6)^2 \end{bmatrix} \quad (1)$$

Where $esd(\varepsilon_i)$ is the estimated standard deviation on the *i-th* component of the strain vector (in Voigt notation), and $cov(\varepsilon_i, \varepsilon_j)$ is the covariance between the strain components *i* and *j*.

The esds and the covariances of the residual strain of uniaxial and cubic inclusions are automatically translated by EntraPT into the full 6 x 6 covariance matrix $\boldsymbol{V}^{\varepsilon}$ of the residual strain. For uniaxial inclusions (i.e. trigonal, tetragonal and hexagonal crystal systems) without symmetry breaking, two normal strain components are equal ($\varepsilon_1 = \varepsilon_2$), while the third ($\varepsilon_3$) is different. The shear components are absent ($\varepsilon_4 = \varepsilon_5 = \varepsilon_6 = 0$). When the residual strain of uniaxial inclusions is determined from Raman spectroscopy through the stRAinMAN program, the strain sum $\varepsilon_1 + \varepsilon_2$ and ε_3 are given as output together with the corresponding uncertainties $esd(\varepsilon_1 + \varepsilon_2)$, $esd(\varepsilon_3)$. The covariance between $\varepsilon_1 + \varepsilon_2$ and ε_3 is also computed and reported as $cov(\varepsilon_1 + \varepsilon_2, \varepsilon_3)$. Given

these parameters, and assuming that $\varepsilon_1 = \varepsilon_2$ are completely correlated, the full covariance matrix of the residual strain $\boldsymbol{V}^{\varepsilon}$ is assembled by EntraPT as:

$$\boldsymbol{V}^{\varepsilon} = \begin{bmatrix} \left(\frac{esd(\varepsilon_1+\varepsilon_2)}{2}\right)^2 & \left(\frac{esd(\varepsilon_1+\varepsilon_2)}{2}\right)^2 & \frac{1}{2}cov(\varepsilon_1+\varepsilon_2,\varepsilon_3) & 0 & 0 & 0 \\ & \left(\frac{esd(\varepsilon_1+\varepsilon_2)}{2}\right)^2 & \frac{1}{2}cov(\varepsilon_1+\varepsilon_2,\varepsilon_3) & 0 & 0 & 0 \\ & & esd(\varepsilon_3)^2 & 0 & 0 & 0 \\ & & & 0 & 0 & 0 \\ & symmetric & & & 0 & 0 \\ & & & & & 0 \end{bmatrix} \quad (2)$$

For cubic crystals without symmetry breaking, the normal strain components are equal $\varepsilon_1 = \varepsilon_2 = \varepsilon_3$, the shear components are absent ($\varepsilon_4 = \varepsilon_5 = \varepsilon_6 = 0$) and the residual volume strain is $\varepsilon_V = \varepsilon_1 + \varepsilon_2 + \varepsilon_3$. Given the uncertainty on the volume strain $esd(\varepsilon_V)$, the full covariance matrix of the residual strain $\boldsymbol{V}^{\varepsilon}$ is:

$$\boldsymbol{V}^{\varepsilon} = \begin{bmatrix} \left(\frac{1}{3}esd(\varepsilon_V)\right)^2 & \left(\frac{1}{3}esd(\varepsilon_V)\right)^2 & \left(\frac{1}{3}esd(\varepsilon_V)\right)^2 & 0 & 0 & 0 \\ & \left(\frac{1}{3}esd(\varepsilon_V)\right)^2 & \left(\frac{1}{3}esd(\varepsilon_V)\right)^2 & 0 & 0 & 0 \\ & & \left(\frac{1}{3}esd(\varepsilon_V)\right)^2 & 0 & 0 & 0 \\ & & & 0 & 0 & 0 \\ & symmetric & & & 0 & 0 \\ & & & & & 0 \end{bmatrix} \quad (3)$$

Once the strains are imported or set in the program, the user can add the *analyses* to the current project.

233

234 **Calculation of the entrapment isomeke with uncertainties**

235 The possible entrapment conditions, i.e. points on the entrapment isomeke (Rosenfeld and Chase,
236 1961; Angel et al., 2014b; Angel et al., 2015b), of each *analysis* can be calculated from the
237 *Calculate Entrapment* tab (Fig 2b). This calculation using isotropic elasticity and the full non-
238 linear EoS of the host and inclusion requires the knowledge of the residual pressure of the inclusion
239 (Angel et al., 2017a). As shown by Bonazzi et al. (2019), when the residual strain of the inclusion
240 is used there are two possible definitions of residual pressure (P_{inc}) for anisotropic inclusions:
241 1) The residual stress can be calculated from the residual strain as:

242

$$\sigma_i = C_{ij}\varepsilon_j \tag{4}$$

243

244 where C_{ij} is the matrix representation in Voigt notation of the 4th rank elastic modulus tensor
245 of the inclusion determined at room conditions. The pressure is then the negative of the mean
246 normal stress:

247

$$P_{inc}^{strain} = -\frac{(\sigma_1 + \sigma_2 + \sigma_3)}{3} \tag{5}$$

248

249

250 2) Alternatively, the residual volume strain can be found as the sum of the normal components of
251 the strain:

$$\varepsilon_V = \varepsilon_1 + \varepsilon_2 + \varepsilon_3 \quad (6)$$

252 from which the residual pressure is obtained using the EoS of the inclusion as:

253

$$P_{inc}^{V} = f_{EoS}(\varepsilon_V) \quad (7)$$

254

255 By default, EntraPT uses model (1) for the calculation of residual pressure. However, the user can
256 enable the *Expert mode* panel from the *Settings* menu and choose model (2) or both the models to
257 explore a comparison of the results (the procedure is explained in details in the Example section
258 of the Supplementary material). The covariance matrix of the residual strain is used to propagate
259 the uncertainties on the calculated residual pressures and the isomekes. If model (1) is selected
260 (eq. 4), the covariance matrix on the residual stress ($\boldsymbol{V^{\sigma}}$) in the inclusion is obtained from that on
261 the residual strain ($\boldsymbol{V^{\varepsilon}}$) as:

$$\boldsymbol{V^{\sigma}} = \boldsymbol{C}\,\boldsymbol{V^{\varepsilon}}\,\boldsymbol{C^{T}} \quad (8)$$

262

263 Where $\boldsymbol{C}$ is the matrix representation in Voigt notation of the 4th rank elastic modulus tensor of the
264 inclusion, and $\boldsymbol{C^T}$ its transpose. Eq. (8) assumes that the uncertainties of the elastic components
265 (usually less than 2% e.g. Lakshtanov et al., 2007) are negligible compared to the uncertainties of
266 the measured strains which are typically larger than 5% (Bonazzi et al., 2019). Moreover, the
267 covariances of the elastic components determined experimentally are often not reported in
268 literature and cannot therefore be used for error propagation.
269 Once the residual stress and its covariance matrix are known, the standard deviation on the residual
270 pressure P_{inc}^{strain} (eq. 5) can be found as:

$$esd(P_{inc}^{strain}) = \frac{1}{3}\sqrt{V_{1,1}^{\sigma} + V_{\mathbf{2},2}^{\sigma} + V_{3,3}^{\sigma} + 2V_{1,2}^{\sigma} + 2V_{1,3}^{\sigma} + 2V_{\mathbf{2},3}^{\sigma}} \quad (9)$$

271

272 On the other hand, if model (2) is selected, the uncertainty on the strain components is propagated
273 into the estimated standard deviation of the volume strain $esd(\varepsilon_V)$ as:

$$esd(\varepsilon_V) = \sqrt{V_{1,1}^{\varepsilon} + V_{\mathbf{2},2}^{\varepsilon} + V_{3,3}^{\varepsilon} + 2V_{1,2}^{\varepsilon} + 2V_{1,3}^{\varepsilon} + 2V_{\mathbf{2},3}^{\varepsilon}} \quad (10)$$

274

275 Given this uncertainty on the volume strain the standard deviation on the residual pressure P_{inc}^{V}
276 (eq. 7) is found as:

$$esd(P_{inc}^{V}) = (1/2)\left[\left|f_{EoS}\left(\varepsilon_V + esd(\varepsilon_V)\right) - f_{EoS}(\varepsilon_V)\right| + \left|f_{EoS}\left(\varepsilon_V - esd(\varepsilon_V)\right) - f_{EoS}(\varepsilon_V)\right|\right] \quad (11)$$

277

278 The calculation of the possible entrapment conditions for the host-inclusion pair is performed
279 assuming isotropic elasticity with the model proposed by Angel et al. (2017a), using the non-linear
280 elasticity of the host and the inclusion. The calculation of the entrapment isomeke is performed
281 calling the specific routines in the Eosfit7n program. Since the calculation of the residual pressure
282 (eq. 4 - 5) requires the elastic tensors ($\boldsymbol{C}$) of each inclusion, which are mostly only known for room
283 *P-T* (1 bar, 25°C), EntraPT is necessarily restricted to calculations from strain measured when the
284 host is at room conditions. The user can set the range of temperatures for the calculation of the
285 entrapment isomeke. The uncertainties on the entrapment isomeke pressuures are estimated from

the standard deviation on the residual pressure $esd(P_{inc})$, by assuming an uncertainty on the residual pressure equivalent to one standard deviation as:

$$P_{inc}^{max} = P_{inc} + esd(P_{inc}) \qquad (12)$$
$$P_{inc}^{min} = P_{inc} - esd(P_{inc})$$

The entrapment isomeke is computed for each value of residual pressure. Therefore, for each temperature step along the isomeke (T_{iso}), P_{iso} is the mean value of the pressure on the isomeke, while P_{iso}^{max} and P_{iso}^{min} are the boundaries on the uncertainty, associated with one standard deviation on the residual pressure. For each T_{iso} on the isomeke the corresponding uncertainty on the P_{iso} is obtained as:

$$esd(P_{iso}) = \frac{1}{2}\left(|P_{iso}^{max} - P_{iso}| + |P_{iso}^{min} - P_{iso}|\right) \qquad (13)$$

Once the calculation is completed, the results of the calculation (residual stress, pressure, P-T points on the entrapment isomekes) of each *analysis* are stored in the current project. An example of the use of EntraPT to calculate the entrapment isomekes of multiple *analyses* is reported in the Supplementary material.

Viewing and plotting data

In the *View Data* tab (Fig. 3) the user can view all of the data relative to each *analysis* and generate relevant plots. The residual strain of one or more *analyses* can be analyzed visually in a scatter plot from the *Plot Strain* page (Fig. 3d). Fig. 3f shows the ε_3 vs ε_1 plot with the strain data measured by Bonazzi et al. (2019) on several quartz inclusions in almandine (the procedures to

generate such plot are described in the Supplementary material). For each *analysis*, the associated confidence ellipse is shown, as obtained from the variance-covariance matrix $\boldsymbol{V}^{\varepsilon}$ determined from the measurement of the residual strain. For a visual reference, the isochors and the lines of isotropic strain and hydrostatic stress state of a crystal of the same phase as the inclusion can be added to the plot (Fig. 3h). The results of the calculation of the entrapment isomeke are shown in the *Results* page (Fig. 3b). The user can also generate a *P*-*T* plot with the isomeke(s) of one *analysis* together with the estimated uncertainty shown as a shaded area from the *Plot Isomekes* page (Fig. 3c and Figs. S5 in the Supplementary material). The isomekes of multiple *analyses* can also be plotted at the same time, even if they belong to different host-inclusion systems. This is particularly useful for constraining the metamorphic conditions if several host-inclusion systems within the same rock were measured. Since some host-inclusion systems are good barometers (e.g. quartz in garnet) while others are good thermometers (e.g. zircon in garnet), the intersection of their isomekes can provide constraints on the *P*-*T* path of the rock (e.g. Zhong et al., 2019).

Export and import of data

Project files, that contain all of the data from all of the *analyses* (elastic properties, strain given as input, covariance matrices, calculation parameters, results, notes etc.) are stored in a database-like format and can be downloaded to the user's computer. Project files can be imported back into EntraPT, to view the data, generate the plots. Importing a project file puts EntraPT in the same configuration as when the project file was created. Once a project is loaded, new *analyses* can be added or existing *analyses* can be deleted. Moreover, multiple project files can be merged in EntraPT to create larger databases. Such project files can be easily shared, making the checking and the comparison of data and results reliable. The project file can be easily imported into MATLAB® and custom scripts can be developed to further process the data and to generate

custom plots, taking advantage that all of the data are structured consistently in the project file. An example of these scripts is included in the Deposit items, and a custom plot generated with it is shown in Fig. S6 of the Supplemental material. During the export procedure from EntraPT, the user can also choose to save the data to spreadsheets that can be read by any commonly used spreadsheet application, such as Microsoft Excel® or LibreOffice®. To preserve the privacy of the users and the complete control of their data, all of the data are deleted from the server when the EntraPT session is terminated and cannot be recovered even by the server administrators. Therefore, downloading the project to the users computer is the only way to have access to the data after the EntraPT session is terminated. The upload and the download of the data to and from the server is always performed over a secure SSL connection.

Implications

EntraPT is a web-based application freely accessible at www.mineralogylab.com/software that provides an easy-to-use tool to calculate entrapment pressures with error propagation from the residual strain measured in mineral inclusions. It obviates the many pitfalls that can arise from manually handling large amounts of data in the multi-step calculations required for elastic geobarometry. EntraPT establishes a consistent workflow to import and visually analyze the measured residual strains, correctly calculate the mean stress in the inclusions, compute the entrapment isomekes with uncertainty estimations and plot the results. With EntraPT all of the data are stored in a consistent format and can be exported as project files and spreadsheets. This allows the data to be shared easily, making the checking and the comparison of data and results reliable. EntraPT will be constantly updated, without requiring the user to download any program. EntraPT is designed on a modular basis, which will allow its functionalities to be expanded in the

350 future, as automated corrections for the geometry of the system and the use of the full elastic
351 anisotropy of the host and the inclusion are developed.

352 **Acknowledgments**

353 We thank Mattia Bonazzi, Nicola Campomenosi, Mattia Gilio, Alice Girani, Joseph Gonzalez,
354 Giulia Mingardi, Marta Morana, Greta Rustioni, Hugo van Schrojenstein Lantman (who also
355 named EntraPT) for comments, data and help in testing the development versions of EntraPT.
356 Laura Brandolini, Marco Cuman, Dario Lanterna and Michelangelo Parvis are thanked for support
357 with the IT infrastructure, the website and the graphical design. Jay Thomas and Guillaume Bonnet
358 are gratefully acknowledged for their positive and useful reviews.

359 This project was supported by the European Research Council (ERC) under the European Union's
360 Horizon 2020 research and innovation programme (grant agreement No 714936 for the project
361 TRUE DEPTHS to M. Alvaro).

362

363 **References**

364 Alvaro, M., Mazzucchelli, M.L., Angel, R.J., Murri, M., Campomenosi, N., Scambelluri,
365 M., Nestola, F., Korsakov, A., Tomilenko, A.A., Marone, F., and others (2020) Fossil subduction
366 recorded by quartz from the coesite stability field. Geology, 48, 24–28.

367 Angel, R.J., Alvaro, M., and Gonzalez-Platas, J. (2014a) EosFit7c and a Fortran module
368 (library) for equation of state calculations. Zeitschrift für Kristallographie-Crystalline Materials,
369 229, 405–419.

Angel, R.J., Mazzucchelli, M.L., Alvaro, M., Nimis, P., and Nestola, F. (2014b) Geobarometry from host-inclusion systems: The role of elastic relaxation. American Mineralogist, 99, 2146–2149.

Angel, R.J., Alvaro, M., Nestola, F., and Mazzucchelli, M.L. (2015a) Diamond thermoelastic properties and implications for determining the pressure of formation of diamond-inclusion systems. Russian Geology and Geophysics, 56.

Angel, R.J., Nimis, P., Mazzucchelli, M.L., Alvaro, M., and Nestola, F. (2015b) How large are departures from lithostatic pressure? Constraints from host–inclusion elasticity. Journal of Metamorphic Geology, 33, 801–813.

Angel, R.J., Mazzucchelli, M.L., Alvaro, M., and Nestola, F. (2017a) EosFit-Pinc: A simple GUI for host-inclusion elastic thermobarometry. American Mineralogist, 102, 1957–1960.

Angel, R.J., Alvaro, M., Miletich, R., and Nestola, F. (2017b) A simple and generalised P–T–V EoS for continuous phase transitions, implemented in EosFit and applied to quartz. Contributions to Mineralogy and Petrology, 172, 29.

Angel, R.J., Murri, M., Mihailova, B., and Alvaro, M. (2019) Stress , strain and Raman shifts. Zeitschrift für Kristallographie-Crystalline Materials., 234, 129–140.

Anzolini, C., Prencipe, M., Alvaro, M., Romano, C., Vona, A., Lorenzon, S., Smith, E.M., Brenker, F.E., and Nestola, F. (2018) Depth of formation of super-deep diamonds: Raman barometry of CaSiO3-walstromite inclusions. American Mineralogist, 103, 69–74.

Ashley, K.T., Steele-MacInnis, M., and Caddick, M.J. (2014) QuIB Calc: A MATLAB® script for geobarometry based on Raman spectroscopy and elastic modeling of quartz inclusions in garnet. Computers and Geosciences, 66, 155–157.

Ashley, K.T., Steele-MacInnis, M., Bodnar, R.J., and Darling, R.S. (2016) Quartz-in-garnet inclusion barometry under fire: Reducing uncertainty from model estimates. Geology, 44, 699–702.

Barron, T.H.K., Collins, J.G., and White, G.K. (1980) Thermal expansion of solids at low temperatures. Advances in Physics, 29, 609–730.

Bonazzi, M., Tumiati, S., Thomas, J.B., Angel, R.J., and Alvaro, M. (2019) Assessment of the reliability of elastic geobarometry with quartz inclusions. Lithos, 350–351.

Campomenosi, N., Mazzucchelli, M.L., Mihailova, B.D., Scambelluri, M., Angel, R.J., Reali, A., and Alvaro, M. (2018) How geometry and anisotropy affect residual strain in host inclusion system: coupling experimental and numerical approaches. American Mineralogist, 103, 2032–2035.

Chopin, C. (1984) Coesite and pure pyrope in high-grade blueschists of the Western Alps: a first record and some consequences. Contributions to Mineralogy and Petrology, 86, 107–118.

Ehlers AM, Zaffiro G, Angel RJ, Boffa-Ballaran T, Carpenter MA, Alvaro M, Ross NL (2020) Thermoelastic properties of zircon: implications for geothermobarometry. American Mineralogist , submitted

Enami, M., Nishiyama, T., and Mouri, T. (2007) Laser Raman microspectrometry of metamorphic quartz: A simple method for comparison of metamorphic pressures. American Mineralogist, 92, 1303–1315.

Gillet, P., Ingrin, J., and Chopin, C. (1984) Coesite in subducted continental crust: PT history deduced from an elastic model. Earth and Planetary Science Letters, 70, 426–436.

Grüneisen, E. (1926) Zustand des festen Körpers. In Drucker C., Ed., Thermische Eigenschaften der Stoffe pp. 1–59. Springer Berlin Heidelberg.

Isaak, D.G., Anderson, O.L., and Oda, H. (1992) High-temperature thermal expansion and elasticity of calcium-rich garnets. Physics and Chemistry of Minerals, 19, 106–120.

Izraeli, E.S., Harris, J.W., and Navon, O. (1999) Raman barometry of diamond formation. Earth and Planetary Science Letters, 173, 351–360.

Jiang, F., Speziale, S., and Duffy, T.S. (2004) Single-crystal elasticity of grossular- and almandine-rich garnets to 11 GPa by Brillouin scattering. Journal of Geophysical Research: Solid Earth, 109.B10

Kohn, M.J. (2014) “Thermoba-Raman-try”: Calibration of spectroscopic barometers and thermometers for mineral inclusions. Earth and Planetary Science Letters, 388, 187-196.

Lakshtanov, D.L., Sinogeikin, S. V., and Bass, J.D. (2007) High-temperature phase transitions and elasticity of silica polymorphs. Physics and Chemistry of Minerals, 34, 11–22.

Mazzucchelli, M.L., Burnley, P., Angel, R.J., Morganti, S., Domeneghetti, M.C.C., Nestola, F., and Alvaro, M. (2018) Elastic geothermobarometry: Corrections for the geometry of the host-inclusion system. Geology, 46, 231–234.

Mazzucchelli, M.L., Reali, A., Morganti, S., Angel, R.J., and Alvaro, M. (2019) Elastic geobarometry for anisotropic inclusions in cubic hosts. Lithos, 350–351.

Milani, S., Nestola, F., Alvaro, M., Pasqual, D., Mazzucchelli, M.L., Domeneghetti, M.C., and Geiger, C.A. (2015) Diamond–garnet geobarometry: The role of garnet compressibility and expansivity. Lithos, 227, 140–147.

Milani, S., Angel, R.J., Scandolo, L., Mazzucchelli, M.L., Ballaran, T.B., Klemme, S., Domeneghetti, M.C., Miletich, R., Scheidl, K.S., Derzsi, M., and others (2017) Thermo-elastic behavior of grossular garnet at high pressures and temperatures. American Mineralogist, 102, 851–859.

Morganti, S., Mazzucchelli, M.L., Alvaro, M., and Reali, A. (2020) A numerical application of the Eshelby theory for geobarometry of non-ideal host-inclusion systems. Meccanica, 1–14.

Murri, M., Mazzucchelli, M.L., Campomenosi, N., Korsakov, A. V., Prencipe, M., Mihailova, B.D., Scambelluri, M., Angel, R.J., and Alvaro, M. (2018) Raman elastic geobarometry for anisotropic mineral inclusions. American Mineralogist, 103, 1869–1872.

Nestola, F., Nimis, P., Ziberna, L., Longo, M., Marzoli, A., Harris, J.W., Manghnani, M.H., and Fedortchouk, Y. (2011) First crystal-structure determination of olivine in diamond: Composition and implications for provenance in the Earth's mantle. Earth and Planetary Science Letters, 305, 249–255.

Özkan, H., Cartz, L., and Jamieson, J.C. (1974) Elastic constants of nonmetamict zirconium silicate. Journal of Applied Physics, 45, 556–562.

Ranganathan, S.I., and Ostoja-Starzewski, M. (2008) Universal elastic anisotropy index. Physical Review Letters, 101, 3–6.

Rodriguez-Carvajal, J., and Gonzalez-Platas, J. (2003) Crystallographic Fortran 90 Modules Library (CrysFML): a simple toolbox for crystallographic computing programs. IUCr Computing Commission Newsletter 1, 50-58.

Rosenfeld, J.L., and Chase, A.B. (1961) Pressure and temperature of crystallization from elastic effects around solid inclusions in minerals? American Journal of Science, 259, 519–541.

Sinogeikin, S. V, and Bass, J.D. (2002) Elasticity of pyrope and majorite-pyrope solid solutions to high temperatures. Earth and Planetary Science Letters, 203, 549–555.

Thomas, J.B., and Spear, F.S. (2018) Experimental study of quartz inclusions in garnet at pressures up to 3.0 GPa: evaluating validity of the quartz-in-garnet inclusion elastic thermobarometer. Contributions to Mineralogy and Petrology, 173, 1–14.

Voigt, W. (1910) Lehrbuch der Kristallphysik. Kristalloptik. Teubner, Leipzig.

Zhang, Y. (1998) Mechanical and phase equilibria in inclusion-host systems. Earth and Planetary Science Letters, 157, 209–222.

Zhong, X., Moulas, E., and Tajčmanová, L. (2018) Tiny timekeepers witnessing high-rate exhumation processes. Scientific Reports, 8, 1–9.

Zhong, X., Andersen, N.H., Dabrowski, M., and Jamtveit, B. (2019) Zircon and quartz inclusions in garnet used for complementary Raman thermobarometry: application to the Holsnøy eclogite, Bergen Arcs, Western Norway. Contributions to Mineralogy and Petrology, 174, 50.

Zhong, X., Moulas, E., and Tajčmanová, L. (2020) Post-entrapment modification of residual inclusion pressure and its implications for Raman elastic thermobarometry. Solid Earth, 11, 223–240.

Zouboulis, E., Grimsditch, M., Ramdas, a., and Rodriguez, S. (1998) Temperature dependence of the elastic moduli of diamond: A Brillouin-scattering study. Physical Review B, 57, 2889–2896.

Captions

Figure 1. Workflow from Raman measurement to the determination of residual strain with stRAinMAN (Angel et al., 2019), and the calculation of the entrapment conditions with EntraPT. The Raman shifts for several modes are measured with Raman Spectroscopy (a). Knowing the Gruneisen tensor of the inclusion and using stRAinMAN (b) the residual strain components of one or several samples are determined and exported as a text file (c). The user imports to EntraPT these strain components (d), sets the host and the inclusion minerals and the parameters of the system (e). Then, with EntraPT the user can analyse the strain states of the inclusions (f) and calculate their residual pressures from the individual components of the strain, using the 4^{th} rank stiffness tensor, or from the volume strain, using the EoS of the inclusion (g). The entrapment isomekes can be calculated and plotted (h), and all the data and results can be exported/imported as project files (i). EntraPT can also be used to process residual strain states measured with X-ray diffraction,

following the steps (d-i) of the workflow. Inputs and outputs to and from the programs are identified by grey and red arrows, respectively.

Figure 2. EntraPT is structured with three main tabs: *Add New Analyses* (a), *Calculate Entrapment* (b) and V*iew Data* (c). The user has first to define one or more new analyses from the *Add New Analyses* tab. Using the panel on the right side the user can set the host and inclusion minerals (d), the geometry (e), the orientation (f) and the measured residual strains (g). This figure shows the Host&Inclusion page (d) where the host and the inclusion minerals are set, and a summary of their EoS is shown to the user.

Figure 3. Under the *View Data* tab the user can view all the data and results in the project, using the *Details* (a), *Results* (b), *Plot Isomekes* (c) and *Plot Strain* (d) pages. Here is shown the visual inspection of the measured residual strains that can be performed from the *Plot Strain* page. The user can select one or more analyses from the *Workspace* (e). In this example, the strain components determined at room temperature for quartz inclusions from experiments Alm-1 and Alm-2 by Bonazzi et al. (2019) are shown. By default, the strain data with their error bars and confidence ellipses are shown in a ε_3 vs ε_1 plot (f), but other choices of axes can also be made. The labels of the analyses, the confidence ellipses, the lines of isotropic strain and hydrostatic stress and the isochors can be shown or hidden (g, h). The range of the axes can be adjusted as needed (i).

518

519

520

Table 1. Equations of State (EoS) and independent components of the at room-conditions elastic (stiffness) tensor of the minerals currently available in the database of EntraPT. For internal consistency, the components of the stiffness tensor from literature were rescaled as described in the main text.

Mineral	Type	EoS from:	C_{ij} (GPa)	C_{ij} modified after:
Almandine	Host/inclusion	Milani et al. (2015)	$C_{11} = 300.2;\ C_{12} = 108.8;\ C_{44} = 93.3;$	Jiang et al. (2004)
Diamond	Host/inclusion	Angel, Alvaro, et al. (2015)	$C_{11} = 1078.4;\ C_{12} = 126.8;\ C_{44} = 575.7;$	Zouboulis et al. (1998)
Grossular	Host/inclusion	Milani et al. (2017)	$C_{11} = 316.7;\ C_{12} = 91.5;\ C_{44} = 102.2;$	Isaak et al. (1992)
Pyrope	Host/inclusion	Milani et al. (2015)	$C_{11} = 291.1;\ C_{12} = 100;\ C_{44} = 93;$	Sinogeikin and Bass (2002)
Zircon	Host/inclusion	Ehlers et al (submitted)	$C_{11} = 422.0;\ C_{12} = 70.0;\ C_{13} = 148.9;\ C_{33} = 488.0;\ C_{44} = 113.1;\ C_{66} = 48.3;$	Özkan et al. (1974)
Quartz	inclusion	Angel, Alvaro, et al. (2017)	$C_{11} = 86.1;\ C_{12} = 7.2;\ C_{13} = 11.7;\ C_{14} = 17.7;\ C_{33} = 105.6;\ C_{44} = 59.2;$	Lakshtanov et al. (2007)

521

522

523

524

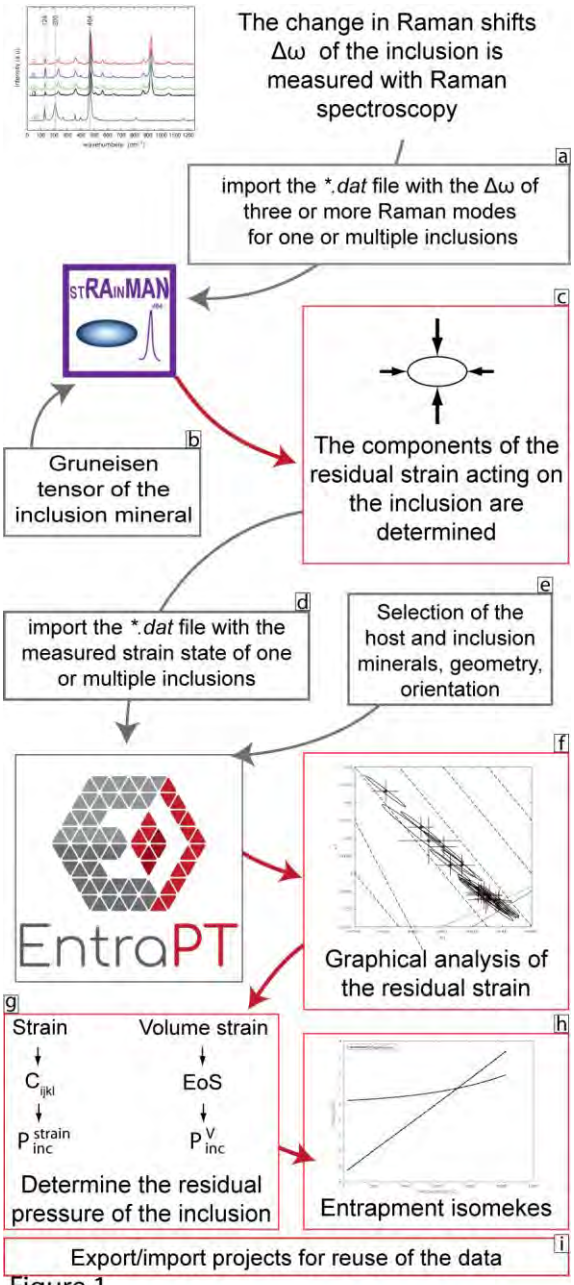

Figure 1

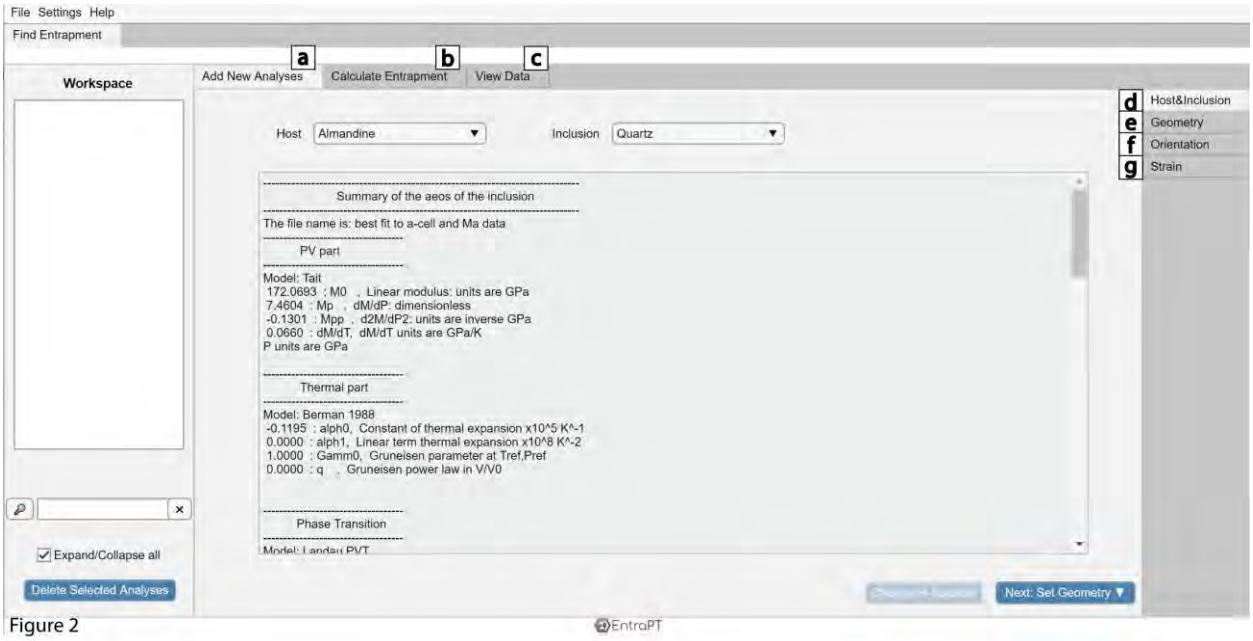

Figure 2

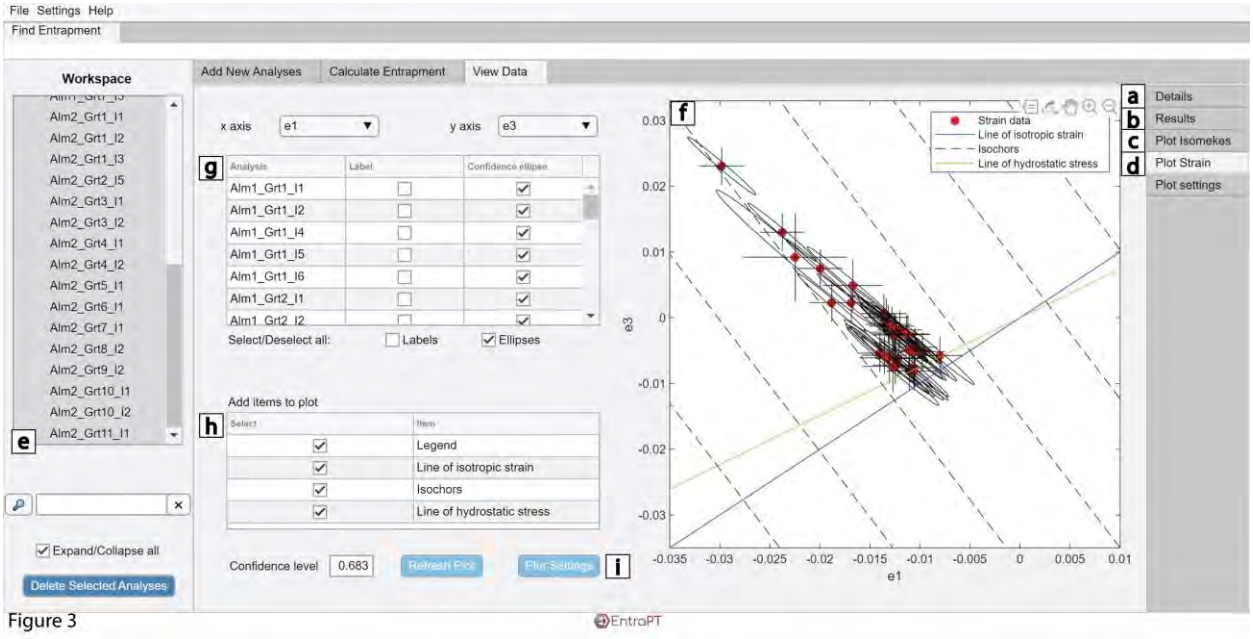

Figure 3

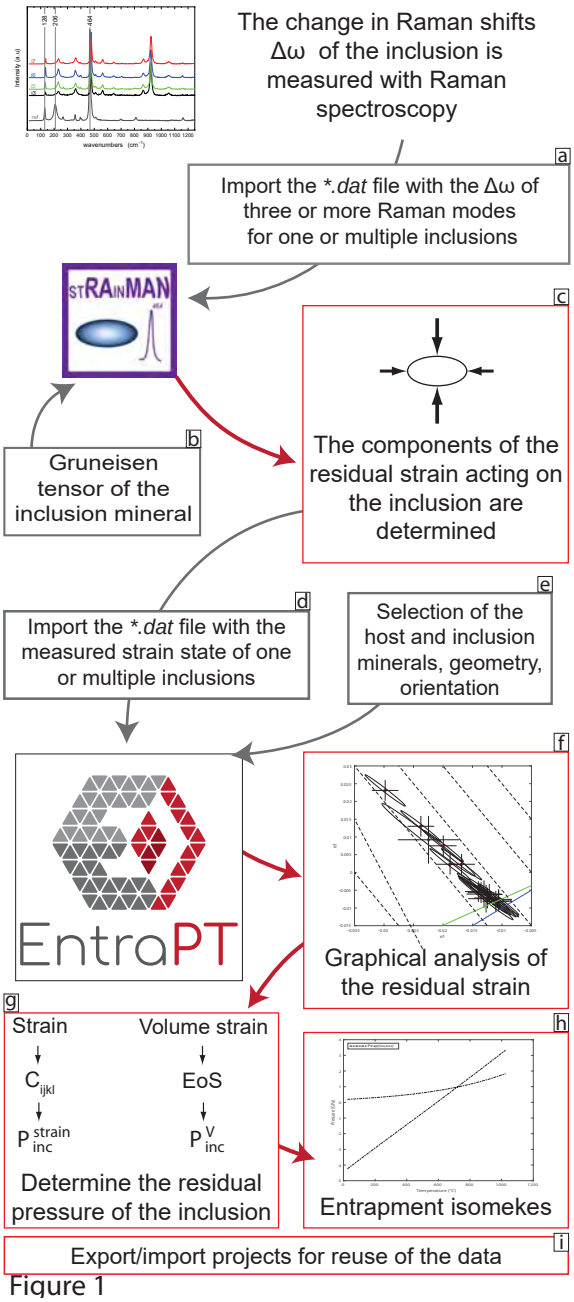

Figure 1

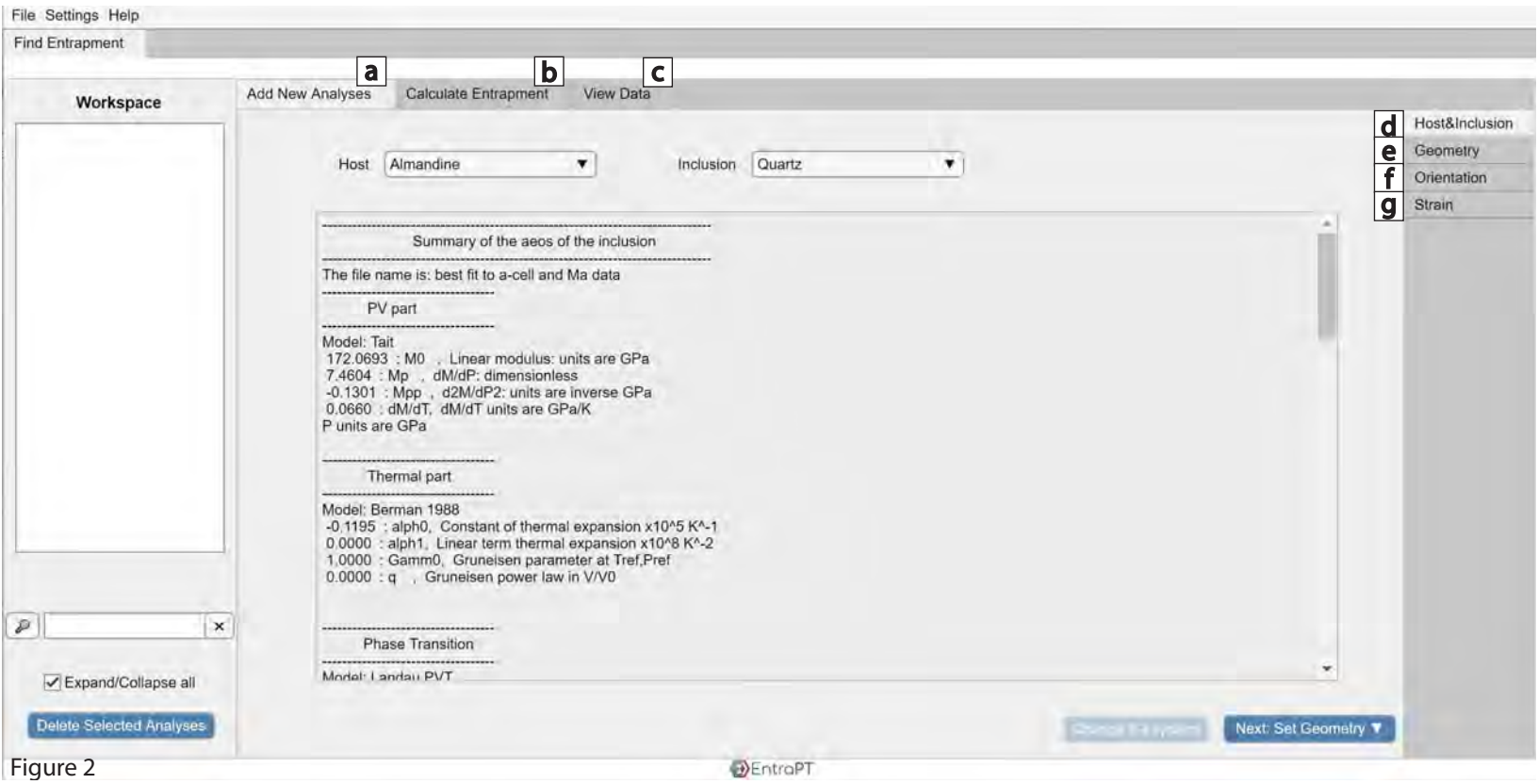

Figure 2

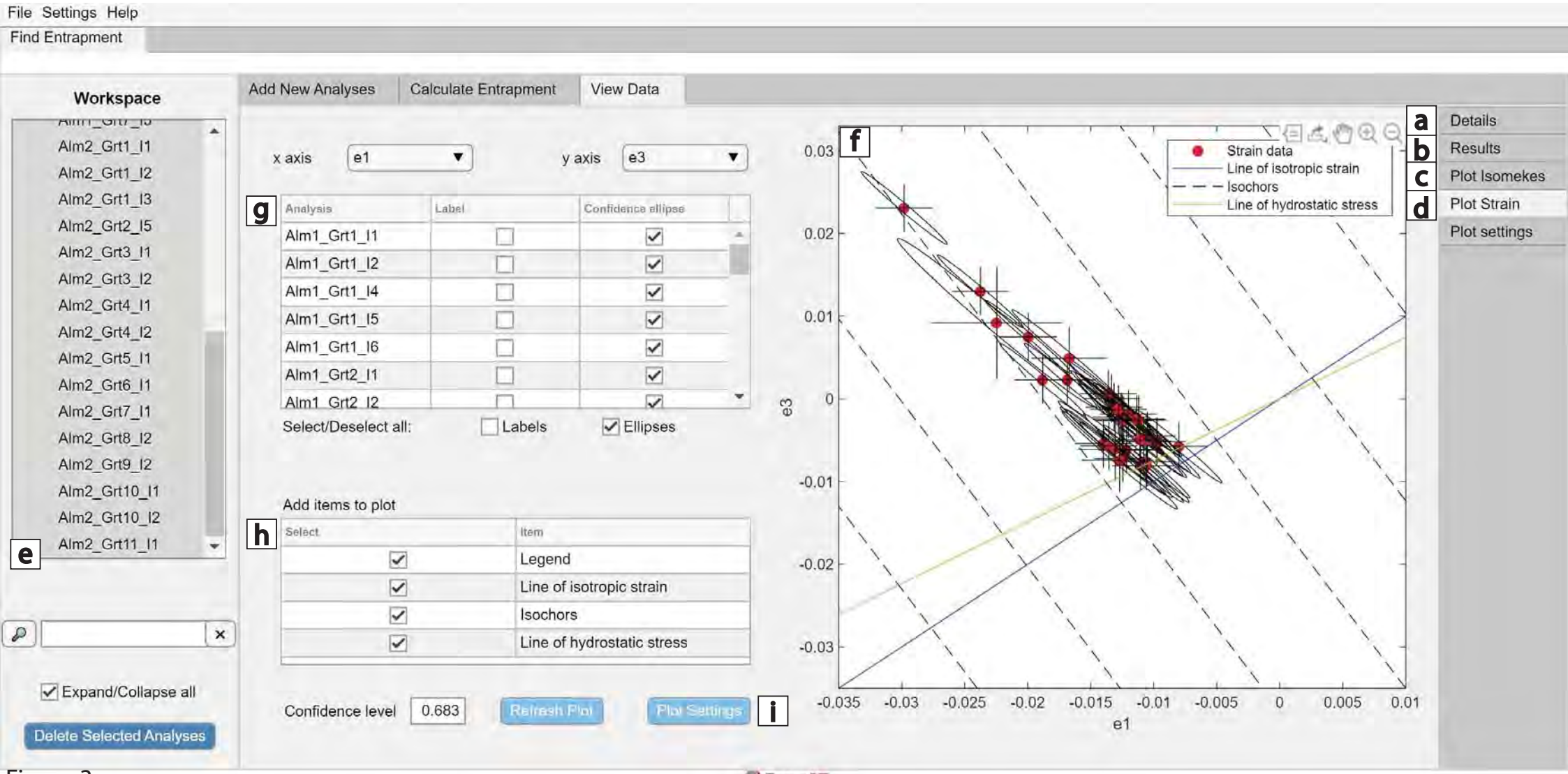

Figure 3